MLM-3658(OP)
CONF-9009256--2

ELUCIDATION OF FUNDAMENTAL PROPERTIES OF HELIUM IN METALS BY NUCLEAR MAGNETIC RESONANCE TECHNIQUES

G. C. ABELL
E.G.&G. MOUND APPLIED TECHNOLOGIES
MIAMISBURG, OHIO, U.S.A.
45342

MLM--3658(OP)

DE91 002715

DISCLAIMER

ABSTRACT

The nuclear magnetic resonance (NMR) properties of very high density ^{3}He in metals are discussed in the context of the corresponding properties in relatively high density bulk ^{3}He. In particular, the effects of ^{3}He diffusion on the contribution of the ^{3}He-^{3}He dipolar interaction to the lineshape and to the spin-lattice relaxation parameter (T_1) are described. It is shown that the temperature dependence of the lineshape and of T_1 are independent sources of information about helium density and also about helium diffusivity. Moreover, T_1 is shown to be a sensitive indicator of melting transitions in bulk ^{3}He. Palladium tritide is presented as a model system for NMR studies of ^{3}He in metals. Experimental NMR studies of this system reveal behavior analogous to what has been observed for bulk helium. Evidence for a ^{3}He phase transition near 250 K is provided by the temperature dependence of T_1. Assuming this to be a melting transition, a density is obtained from the bulk helium EOS that is in good agreement with theory and with swelling measurements on related metal tritides. ^{3}He NMR measurements have also provided information about the density distribution, helium diffusivity, and mean bubble size in palladium tritide.

I. INTRODUCTION

Nuclear magnetic resonance (NMR) is, in principle, an ideal technique for studying ^{3}He in metals. If the helium concentration is sufficient to overcome the inherent sensitivity limitation of NMR ($\sim 10^{18}$-10^{19} spins) and if the host metal is nonmagnetic, then NMR experiments can be expected to provide significant information about the properties of ^{3}He in that particular host. Because of the sensitivity limitation, materials containing ^{3}He via ion-implantation are difficult to study. This is illustrated by the work of Weaver, et al [1] on ion-implanted Pd, in which a specially designed NMR probe cooled by liquid helium provided a limited amount of information. For this reason, most NMR studies of ^{3}He in metals have been performed on metal tritides, in which the helium is implanted with very little kinetic energy by triton decay ($\simeq$ 12 year half-life). A homogeneous tritide will result in homogeneous deposition of ^{3}He. A typical metal tritide requires about five months of decay before a useful ^{3}He signal is obtained. Because of the radiolytic hazards associated with tritium, either special containment or sample preparation procedures will generally be required.

The ^{3}He NMR studies of Bowman [2] on the tritides of lithium, titanium, and uranium illustrate the "tritium trick" approach. However, these materials are not necessarily representative of helium in metals; certainly not LiT, which is an ionic salt. The only one of these for which a temperature-dependent NMR study was performed was UT_3 [3] which, unfortunately, is ferromagnetic below about 200 K. Consequently, the magnetic properties of ^{3}He are obscured in this crucial temperature range. Nonetheless, this work did provide microscopic evidence that the ^{3}He was in bubbles and not on host lattice interstitial sites. The transmission electron microscopy (TEM) work of Thomas and Mintz [4] on palladium tritide ($PdT_{0.6}$) provided the first direct images of bubbles in a metal tritide. Since then, bubbles have been imaged in several other tritides as well [5].

Subsequent to the TEM work on $PdT_{0.6}$, NMR studies of ^{3}He in palladium tritide by Abell and Attalla [6] provided evidence for a melting transition near 250K and also provided information about helium diffusivity in solid high-density helium. The density obtained from the observed melting temperature using the bulk helium equation-of-state (EOS) was consistent with theoretical predictions of Wolfer [7] and also with densities inferred from dilatometry measurements on the tritides of Nb and Ta [8]. After additional aging of the palladium tritide material, detailed NMR analysis revealed a range of melting temperatures, from which a distribution of densities could be inferred [9]. This work demonstrated the potency of the NMR technique for providing fundamental information about ^{3}He in metals.

The present article describes the observed NMR behavior of ^{3}He in palladium tritide, which is used as a model system to illustrate the kind of information about ^{3}He in metals that can be obtained via NMR. The article begins with a description of the NMR behavior of <u>bulk</u> ^{3}He as it relates to the corresponding behavior of ^{3}He in metals. The underlying theory is briefly reviewed in order to explain the effects of motion on NMR relaxation and lineshape parameters, and to illustrate the different motional regimes. Against this backdrop, the NMR behavior of ^{3}He in palladium tritide is then described in relation to such fundamental properties as density and self-diffusion. Hydrogen isotope effects on ^{3}He lineshape and T_1 parameters in palladium tritide, due to interaction of ^{3}He with hydrogen at the bubble surface, are also discussed.

II. NMR BACKGROUND.

If surface effects can be ignored, the NMR properties of ^{3}He in highly pressurized nm-bubbles should be essentially those of bulk ^{3}He of comparable density. For bulk densities greater than about 0.056 moles/cm^3, the helium-helium exchange interaction [10] is unimportant, and the bulk NMR behavior is dominated by the dipolar interaction between the nuclear spins and by the modulation of this interaction due to diffusive motion. The NMR properties of bulk ^{3}He in this diffusive regime have been determined for a range of densities up to a maximum density of only about 0.060 moles/cm^3. (The density of ^{3}He in bubbles is $\approx$0.2 moles/cm^3 [6, 8].) Nonetheless, the theoretical understanding of NMR characteristics for this relatively simple system provides the basis for prediction of certain properties at much higher densities than have been observed for bulk ^{3}He. The point of departure for understanding the NMR properties of bulk ^{3}He is the Hamiltonian for a system of interacting spin-1/2 nuclei in a uniform magnetic field [11]:

$$H = H_Z + H_D. \tag{1}$$

The term

$$H_Z = -\gamma\hbar H I_z \tag{2}$$

is the Zeeman interaction of the spin system with an external magnetic field of magnitude H directed along the z-axis. The quantity γ is the gyromagnetic ratio of a ^{3}He nucleus, while I_z represents the component of the total spin angular momentum along the external field direction and $\hbar$ is Planck's constant divided by 2π. The last term in eqn. (1) is the dipolar interaction, i.e., coupling of a spin to the magnetic dipole fields of neighboring spins, for which the classical expression is

$$H_D = \Sigma[\mu_i\cdot\mu_j/(r_{ij})^3 - 3(\mu_i\cdot r_{ij})(\mu_j\cdot r_{ij})/(r_{ij})^5]. \tag{3}$$

In this equation, the quantity μ_i is the magnetic moment of nucleus i, r_{ij} is the internuclear vector between nuclei i and j, and the sum is over all distinct pairs of nuclei. In most NMR studies, H_D is much smaller than H_Z and is accurately treated by perturbation theory.

It is clear from the form of eqn. (3) that motion of the nuclei will modulate the dipolar interaction. At low enough temperatures, the motion will be sufficiently slow that only the instantaneous value of H_D will be relevant. The effect of H_D in this case is to broaden the spectrum relative to that for free spins. This regime is called the rigid- or static-lattice limit; linewidth analysis in this limit provides structural information. For fast isotropic motion, $\langle H_D\rangle = 0$ (the angular brackets here denote an appropriate time-average) in first order and to this extent, there is no broadening. Fluctuations of H_D represent second-order effects which provide a mechanism for spin-lattice (T_1) relaxation. This latter regime is the motionally narrowed limit; a study of T_1 in this limit provides dynamical information.

The way in which these different regimes fall out of the Hamiltonian (1) is best appreciated by expressing the dipolar interaction in terms of spin operators. H_D then consists of six quantum-mechanical operators for each pair of nuclei, having the

form:

$$O_{ij} = R_{ij} I_{ij}. \tag{4}$$

These operators have matrix elements connecting nuclear Zeeman states (the eigenstates of H_Z) which differ in total magnetic spin quantum number m by either 0, 1, or 2. Each operator O_{ij} is a product of a spin function I_{ij} (which is itself a product of a spin operator for nucleus i with one for nucleus j) and a spatial function R_{ij}, which depends on the length and orientation relative to the external field H of $\underline{r}_{ij}$. For sufficiently slow motion, it is the instantaneous value of H_D that matters; in this static-lattice limit, only the $\Delta m=0$ matrix elements (i.e., the secular or first-order terms) of the O_{ij} operators are important in the overall Hamiltonian (1). If there were no dipolar interaction (i.e., $H_D=0$), the spectrum--which includes all possible transitions with $\Delta m=1$--would consist of a single line at the Larmor frequency, defined as:

$$\omega_0 = \gamma H. \tag{5}$$

When $H_D \neq 0$ (i.e., the case of static dipolar coupling) the spectrum is broadened out about ω_0. The broadening is due to the multiplicity of values that the secular perturbation can assume as a consequence of its dependence on spin operators for each nucleus in the coupled array (the spin quantum number for each ^{3}He nucleus is $\pm 1/2$). Moreover, in a polycrystalline sample, the $\underline{r}_{ij}$ are distributed randomly in all directions, resulting in a smeared out spectrum even for a two-spin system.

Apart from special cases, there is no exact solution for the Hamiltonian of eqn. (1) in the static-lattice limit. Thus an exact solution of the resonance shape is not possible in this limit. Nonetheless, the method of moments introduced by Van Vleck [12] allows a determination of properties of the resonance line without explicit determination of the eigensolutions. Thus in the case of equivalent ^{3}He spins, the second moment of the resonance lineshape, which is defined very generally as

$$M_2 = \int_{-\infty}^{\infty} (\omega-\omega_0)^2 g(\omega) d\omega, \tag{6}$$

($\omega g(\omega)$ is the lineshape function) is determined precisely by the method of moments to be

$$M_2 = (9/16)\gamma^4 \hbar^2 \Sigma_k (1-3\cos^2\theta_{jk})^2/(r_{jk})^6. \tag{7}$$

In this expression, M_2 is in frequency units and θ_{jk} is the angle between $\underline{r}_{jk}$ and the external field.

The lattice sum in eqn. (7) has been determined for various infinite lattice structures [13], and can be expressed either in units of $1/a^6$ (a being the lattice parameter) or in units of ρ^2, where ρ is the ^{3}He density. When expressed in terms of ρ, the lattice sum is nearly independent of structure. The remaining quantities in eqn. (7) are precisely known, and for ^{3}He in a close-packed structure

$$M_2 = 544.5\rho^2, \tag{8}$$

with M_2 in units of Gauss^2 (the conversion between Gauss and frequency units is given by eqn. (5)) and ρ in mole/cm^3. The experimental determination of M_2 is relatively straightforward, once it is demonstrated that the static-lattice limit has been achieved. A good example of the use of M_2 to obtain structural information is the proton NMR work of Bowman, et al [14] on zirconium hydride.

The effects of motion due to self-diffusion of the ^{3}He nuclei on the Hamiltonian given by eqn. (1) will now be described, following the work of Schlichter [11]. The motion is characterized by a correlation time τ which is essentially the time between diffusive hops. It is appropriate here to define more precisely the criterion for distinguishing the static-lattice (large τ) and motionally-narrowed (small τ) regimes. Clearly there is an intermediate range for τ corresponding to a crossover between these two motional regimes. This crossover regime, which is difficult to characterize quantitatively, is defined by the condition

$$\omega_d \tau = 1, \tag{9}$$

where $\omega_d = \sqrt{M_2}$ is a frequency characterizing the strength of the dipolar interaction. The changeover from the broad static-lattice line to a relatively narrow line generally occurs over a small range of values for τ. For thermally activated diffusion

$$\tau = \tau_0 \exp(W/T), \tag{10}$$

where $W = E_a/k$ is the activation energy in units of degrees Kelvin and τ_0 is the correlation time in the high-temperature limit. Substitution of eqn. (10) into eqn. (9) gives the temperature, T_N, at which the narrowing condition expressed by eqn. (9) is satisfied:

$$T_N = -W/\ln(\omega_d \tau_0). \tag{11}$$

In the case of fast <u>isotropic</u> motion satisfying the condition $\tau \ll (\omega_d)^{-1}$, the secular terms (terms in H_D which produce first-order effects) get averaged to zero. Thus, the relevant zero-th order description is one of non-interacting spins, viz. the eigensolutions of the Zeeman Hamiltonian (eqn. (2)). Components of the fluctuating dipolar field (the dipolar field is defined by eqn. (3)) which are <u>transverse</u> to the static field H, can cause changes in the ensemble-averaged nuclear spin magnetization parallel to the static field, i.e., change in $\langle M_z \rangle$. A good analogy for this effect is the manipulation of $\langle M_z \rangle$ by an applied rf-field transverse to the static field (this is the "experimental handle" in pulsed NMR experiments). But this is a resonance phenomenon--the applied rf must provide a magnetization vector which rotates in the transverse plane <u>at the Larmor frequency</u> ω_0, defined by eqn. (5), in order to give a finite probability for transitions between Zeeman states. These latter transitions are ultimately behind any changes in $\langle M_z \rangle$. In the same way, transverse components of the fluctuating dipolar field which are precessing at ω_0 provide a mechanism for changing $\langle M_z \rangle$. This relaxation process involves a transfer of energy between the spin system and the phonon modes associated with self-diffusion; it is thus a spin-lattice or T_1 process. The relaxation will be most efficient when the amplitude at ω_0 of the Fourier spectrum of the fluctuating dipolar field is optimum. This occurs when $\omega_0 \tau \approx 1$ and is manifested by a minimum value for T_1 as a function of τ

(i.e., as a function of temperature--see eqn. (10)). Quantitative analysis of this relaxation mechanism gives the result [10]

$$1/T_1 = (2M_2/3)[\tau/(1+\tau^2\omega_0^2) + 4\tau/(1+4\tau^2\omega_0^2)]. \qquad (12)$$

The magnitude of T_1 at the minimum is determined as an extremum of this equation to be

$$(T_1)_{min} = 1.05\omega_0/M_2. \qquad (13)$$

If there are no additional relaxation mechanisms in play, it follows from equations (8) and (13) that determination of $(T_1)_{min}$ provides a measure of the density. Determination of T_1 as a function of temperature provides dynamical information via the parameter τ in eqn. (12). It is clear that a discontinuous change in τ will be manifested as a discontinuity in T_1. A ^{3}He melting transition involves abrupt changes in the concentration and mobility of vacancies, which determine ^{3}He self-diffusion. For bulk ^{3}He, T_1 increases by a factor of $\simeq 10^3$ in going from the solid to the liquid phase [15]. It follows that a study of T_1 as a function of the appropriate intensive variable (P or T in the case of ^{3}He) can be used to monitor the melting transition. The work of Holcomb and Norberg [16] illustrates the study of the temperature-dependence of T_1 as a means of obtaining information about self-diffusion in alkali metals, which--just as for solid ^{3}He--is via a vacancy mechanism. A similiar study of self-diffusion in bulk solid ^{3}He [17] shows that the diffusion activation energy W is a monotonically increasing function of density.

III. NMR Properties of ^{3}He in Palladium Tritide.

A. Effects due to ^{3}He-^{3}He dipolar interaction.

The NMR behavior of bulk solid ^{3}He as described above provides a background for the following discussion of the observed NMR behavior of ^{3}He in aged palladium tritide [6],[9],[18],[19]. Figure 1 shows the ^{3}He spin-lattice relaxation parameter (T_1), represented by the filled circles, as a function of temperature in 1-year-old $PdT_{0.6}$ (He/Pd atomic ratio $\simeq$ 0.030). The major feature in fig. 1 is the abrupt change in T_1 near 250 K. Assuming that this is due to a solid/fluid melting transition and assuming that the bulk helium equation-of-state (EOS) applies, the helium density (ρ) is found to be 0.20 cm^3/mole. Another important feature in fig. 1 is the existence of a minimum for T_1, which could be a consequence of activated diffusive motion modulating the ^{3}He dipolar interaction. If so, then equation (12) allows τ (essentially, the time between diffusive hops) to be determined from the T_1 data. The results of this latter analysis are represented in fig. 1 by the solid triangles, which correspond to τ^{-1}, shown on the right-hand scale. From eqn. (10), the slope of the semilog plot of τ^{-1} vs. 1/T gives an activation energy of 0.032 eV (i.e., W=370 K) for the ^{3}He self diffusion. This result is consistent with an extrapolation from much lower densities of the density dependence of W determined for bulk solid ^{3}He [6], [17].

A significant test of the hypothesis that the relaxation mechanism is diffusive modulation of the dipolar interaction is provided by eqn. (11), which allows a prediction of the characteristic temperature for motional narrowing, T_N. Using the Arhennius parameters obtained from the fit of the solid triangles in fig. 1 to the inverse of eqn. (10), and a value for M_2 obtained from eqn. (8) with ρ=0.20 moles/cm^3 (remembering that $\omega_d = \sqrt{M_2}$), eqn (11) gives the result

T_N=34±5 K. Figure 2 shows the measured ^{3}He linewidth at $\omega_0/2\pi$=143MHz [18] as a function of temperature in palladium containing He/Pd=0.3. (This material was aged ≈8 years as a tritide ($PdT_{0.6}$), and then detritided by ambient temperature evacuation [19].) Abrupt narrowing is observed to occur in the range 30-45K, which agrees with the predicted result. Analysis of the static-lattice lineshape at 4 K provides a value for M_2 which, when substituted in eqn. (8), gives the result ρ=0.18 moles/cm^3. (The correction for finite bubble size is presumed to be small.) The accuracy of this result is probably no better than about ±0.03, due to a fairly large correction for magnetic susceptibility effects in palladium metal. (The broadening due to susceptibility effects scales with ω_0, whereas that due to the dipolar interaction is independent of ω_0.) Melting temperature information obtained from a study of T_1 vs. temperature for the same sample [18] indicates that the mean ^{3}He density is about 0.15 moles/cm^3, which agrees reasonably well with the determination from the lineshape analysis. (Note that while the prediction for T_N given earlier was based on ρ=0.20 moles/cm^3, W is not a strong function of ρ so that the predicted T_N is reduced only to about 30 K using ρ=0.15 moles/cm^3.) These results constitute very strong evidence that for $T < T_m$, the NMR behavior of ^{3}He in palladium tritide is essentially that expected for bulk ^{3}He at a comparable density.

There is one difficulty in the results described thus far: using eqns. (8) and (13), the observed magnitude of T_1 at the minimum in fig. 1 gives $\rho \approx 0.13$ moles/cm^3 for the one-year-old palladium sample. This result is significantly smaller than the value of 0.20 moles/cm^3 obtained from T_m. The discrepancy in the density is more apparent than real because, as will be shown, the melting temperature information implies a moderately broad distribution of densities. Thus by eqns. (8), (10), and (12), and the fact that W depends on ρ, there is a corresponding distribution of T_1's. The observed T_1 minimum, obtained from the superposition of the different T_1's--each with its own minimum--can be appreciably larger than the result given by eqn. (13) using the mean density. The difficulty is that eqns. (8) through (13) are based on the assumption of homogeneity; thus they require modification to take the density distribution into account. For eqn. (8), this amounts to using $\langle\rho^2\rangle$ in place of ρ^2, but for the other equations the modifications are not so straightforward. Nonetheless, so long as the distribution is not too broad, the behavior is qualitatively the same as for a homogeneous system.

The evidence for a distribution of densities in the one-year-old palladium sample is that between 200 and 280K, T_1 is strongly nonexponential, whereas outside this range it is ostensibly exponential. Moreover, the nonexponential T_1's are well described by a sum of two exponentials having the characteristics of the two phases outside this range. Figure 3 shows T_1 data taken for the same sample shown in fig. 1 after aging for two years (He/Pd=0.060), and includes the results from a two-exponential fit in the mixed phase region. The observed dependence of T_1 on ω_0 in the solid phase is consistent with eqn. (13). From the T_1 analysis, one also gets the mole fraction of ^{3}He in each phase as a function of temperature. Figure 4 shows the fluid phase fraction vs. temperature for the two-year-old material. Figure 5 compares a distribution function derived from the information in figure 4 [9] using the bulk EOS with one obtained in a similiar manner for the Pd material with He/Pd=0.3 (the 8-year-old Pd). Because of the approximations involved in the analysis, the distributions shown in fig. 5 are fairly crude representations of the actual distributions. In fact, a bimodal distribution would not be inconsistent with the observed ^{3}He melting behavior in the

two different samples. The existence of a distribution of densities is confirmed for the 8-year-old sample by the observation [18] of coexisting broad and narrow ^{3}He lineshape components in the temperature range (30-45K) where motional-narrowing occurs (see figure 2). This observation is understood by recognizing that eqn. (11) implies a distribution for T_N corresponding to that for ρ.

The evolution of the density distribution with age (i.e., -He/Pd atomic ratio) in palladium tritide is represented in figure 6, which shows the range of melting temperatures as a function of age. It is clear from figures 5 and 6 that the distribution broadens with age and shifts to lower densities. The mean density obtained from the data in fig. 6 systematically decreases with age, from a value of 0.21 moles/cm^3 when He/Pd=0.017 (0.55-year-old sample), to a value of 0.15 moles/cm^3 when He/Pd=0.3 (8-year-old sample).

3. Effects due to ^{3}He interactions with unlike spins.

Calorimetry measurements reveal [19] that when aged palladium tritide is evacuated at ambient temperature, an amount of tritium remains absorbed in the material considerably in excess of the expected amount based on the known solubility of tritium in unaged palladium [20]. Figure 7 is a plot of the excess absorbed tritium as a function of He/Pd atomic ratio; it reveals that the concentration of excess tritium ($[T]_{xs}$ is defined as the T/Pd atomic ratio in excess of the equilibrium solubility ratio) scales with the 2/3-power of the ^{3}He concentration. This result suggests that $[T]_{xs}$ is associated with the bubble surface. Assuming trapping at the bubble/metal interface, $[T]_{xs}$ for the sample with He/Pd=0.0050 corresponds to a "surface coverage" of ≈3-4 monolayers. This estimate uses the TEM determination of bubble size in a comparably-aged palladium tritide [4].

If a large fraction of the excess tritium is in close proximity to the bubbles, then the tritium nuclei can influence the ^{3}He NMR behavior through the ^{3}H-^{3}He dipolar interaction (given also by eqn. (3)). An important factor in this regard is that ^{3}H has the largest magnetic moment of any nucleus. But how can one determine whether or not the ^{3}He NMR is influenced by the ^{3}H spins? Exchange of hydrogen isotopes in palladium at near ambient temperatures is straightforward [21] and, because $\gamma(^2H)/\gamma(^3H)\approx 0.2$, replacement of tritium by deuterium will greatly diminish the hydrogen-helium dipolar coupling.

Figure 8 compares the ^{3}He lineshape at 300 K (8a) and the temperature dependence of the ^{3}He T_1 (8b) before and after replacement of tritium by deuterium in $PdT_{0.07}{}^3He_{0.3}$ (8-year-old palladium tritide sample). These results provide strong microscopic evidence that a significant fraction of the tritium is in close proximity to the helium bubbles. The observation at 300 K of significant lineshape effects due to ^{3}H-^{3}He dipolar coupling is not inconsistent with rapid ^{3}He motion, given the highly anisotropic nature of the motion.

An analysis, using a continuum approximation, of the problem of ^{3}He spins interacting with ^{3}H spins trapped at the bubble surface [22] predicts that if both spin species are highly mobile, the secular terms from the dipolar interaction average to zero. Thus, in this limit, a hydrogen isotope effect on the ^{3}He lineshape is not expected. However, in the limit of highly mobile ^{3}He spins and static ^{3}H spins, the analysis predicts a residual broadening with a second moment given by:

$$\langle (M_2)_{IS} \rangle = (8\pi^2/15)(\hbar\gamma_I\gamma_S)^2(N_S/N_I)\rho_I/r^3, \tag{14}$$

where I,S refer to ^{3}He, ^{3}H spins respectively and r is the radius of the shell of trapped tritium spins (presumed to be trapped at the bubble surface). The angular brackets on the left-hand side of eqn. (14) denote a time-averaging over the motion of the I spins. Using in eqn (14) the values N_S/N_I=0.25 (from figure 7), ρ_I=10^{23} spins/cm^3 (^{3}He atomic density), and $\langle (M_2)_{IS} \rangle$=6±4x$10^7$ sec^{-2} obtained from an analysis of the lineshape information in figure 8a, gives the result r=1.0±0.2nm for the 8-year-old material. This value of r seems to be on the low side; it may be that the ^{3}He mobility is not large enough to give complete averaging. This question can presumably be resolved by a temperature-dependent study of the lineshape effect. Given that $\rho_I/N_I \propto r^{-3}$ and assuming that $N_S \propto r^2$ (see figure 7), eqn. (14) predicts that $\langle (M_2)_{IS} \rangle$ scales with $1/r^4$. The residual dipolar broadening of the ^{3}He lineshape by surface-trapped hydrogen should therefore provide a fairly sensitive probe of mean bubble size.

The continuum analysis also provides an estimate, similiar to eqn. (13), for the optimum spin-lattice relaxation available from the IS-dipolar interaction:

$$(T_1)_{IS} > \omega_0/(M_2)_{IS}. \tag{15}$$

In this expression, $(M_2)_{IS}$ is the contribution of the helium-hydrogen dipolar interaction to the second moment of the helium lineshape in the limit when both spin species are static. It is given by [22]

$$(M_2)_{IS} = (\pi/30)(\hbar\gamma_I\gamma_S)^2(N_S/N_I)\rho_I/d^3, \tag{16}$$

where d is the separation between the outermost ^{3}He layer and the innermost shell of trapped tritium spins. The observed behavior of $(T_1)_{IS}$, deduced from figure 8b using

$$1/T_1(^3H) = 1/T_1(^2H) + 1/(T_1)_{IS}, \tag{17}$$

is consistent with d < 0.25nm, which supports the hypothesis that the tritium is trapped at the bubble/metal interface.

The above results indicate that experimental determination of the effects of either ^{3}H or ^{1}H spins (the magnetic properties of ^{1}H are very similiar to those of ^{3}H), on ^{3}He lineshape and relaxation parameters can provide information about bubble geometry and about dynamics of hydrogen species trapped at the bubble surface. However additional experimental work is needed to establish these results.

IV. Conclusions

This review has attempted to demonstrate the utility of ^{3}He NMR for providing fundamental information about helium in metals. Information about helium density and mobility has been obtained from measurements of ^{3}He lineshape and spin-lattice relaxation time parameters. Bubble size information and information related to hydrogen trapped at the bubble/metal interface have been obtained by studying hydrogen isotope effects on the ^{3}He NMR behavior. While fundamental characterization of helium in metals via ^{3}He NMR has for the most part been limited to the palladium tritide

system, the technique should be useful for other systems as well. The tritides of group IV and V metals in particular should be viable candidates. Because of the inherent sensitivity limitation of NMR, study of ion-implanted materials will be more difficult. Application to ferromagnetic materials will be limited to temperatures above the Curie transition. There is probably much that can be gained by extending the technique. In particular, implementation of magic angle sample spinning and double resonance techniques may allow more detailed characterization of helium in favorable systems such as palladium tritide.

Acknowledgements

The author acknowledges the contributions of D. West, D. Kirk, L. Matson, W. Tadlock, W. Rodenburg, R. Yauger, R. Baker, and A. Attalla of E.G.&G. Mound to various aspects of the experimental effort. EG&G Mound Applied Technologies is operated by EG&G for the U.S. Department of Energy under Contract No. DE-AC04-88DP43495.

REFERENCES

[1] H.T.Weaver and W.Beezhold, Appl.Phys.Lett. 24 522(1974).
[2] R.C.Bowman, Jr., Nature 271 531(1978).
[3] R.C.Bowman, Jr. and A.Attalla, Phys.Rev.B16 1828(1977).
[4] G.J.Thomas and J.M.Mintz, J.Nucl.Mater.116 336(1983).
[5] T. Schober and R. Lasser, J. Nucl. Mat. 120, 137(1984); see also R. Lasser, in Tritium and Helium-3 in Metals, (Springer-Verlag, Berlin, 1989) ch. 6.
[6] G.C.Abell and A.Attalla, Phys.Rev.Lett.59 995(1987).
[7] W.G.Wolfer, Phil.Mag A58 285(1989).
[8] T.Schober, J.Golczewski, R.Lasser, C.Dieker, and H.Trinkaus, Z.Phys.Chem.147 161(1986).
[9] G.C.Abell and A.Attalla, Fusion Technol.14 643(1988).
[10] A.Abragam and M.Goldman, Nuclear Magnetism: Order and Disorder, Clarendon, Oxford 1982 ch.3.
[11] C.P.Slichter, Principles of Magnetic Resonance, Springer-Verlag, Berlin 1978 ch.3, ch.5.
[12] J.H.Van Vleck, Phys.Rev.74 1168(1948).
[13] H.S.Gutowsky and B.R.McGarvey, J.Chem.Phys.20 1472(1952).
[14] R.C.Bowman,Jr., E.L.Venturini, and W.-K.Rhim, Phys.Rev.B.26 2652(1982).
[15] H.A.Reich, Phys.Rev.129 630(1963); R.L.Garwin and A.Landesman, Phys.Rev.133 A1503(1964).
[16] D.F.Holcomb and R.E.Norberg, Phys.Rev.98 1074(1955).
[17] N.Sullivan, G.Deville, and A.Landesman, Phys.Rev.B11 1858(1975).
[18] G.C.Abell and D.F.Cowgill, submitted for publication.
[19] R.C.Bowman, Jr., G.Bambakidis, G.C.Abell, A.Attalla, and B.D.Craft, Phys.Rev.B37 9447(1988).
[20] R.Lasser, J.Less-Common Met.131 263(1987); R.Lasser, Phys.Rev.B29 4765(1984).
[21] W.M.Rutherford, in Hydrogen Storage Materials, edited by R.G.Barnes, Mater. Sci. Forum Series, Vol.31(Trans Tech Publications, Aedermannsdorf, Switzerland, 1988),p.19.
[22] G.C.Abell and G.Bambakidis, unpublished work.

FIGURE CAPTIONS

Figure 1. Temperature dependence in 1-year-old $PdT_{0.6}$ of ^3He T_1 relaxation time (filled circles, left-hand scale) at 25 MHz; and of ^3He jump frequency τ^{-1} (filled triangles, right-hand scale) obtained from the T_1 data via eqn. (12).

Figure 2. Spectral linewidth of ^3He in 8-yr-old PdT_x as a function of temperature ($\omega_0/2\pi$ = 142.8MHz).

Figure 3. Temperature dependence of ^3He T_1 in 2-year-old $PdT_{0.6}$ at 45.7 MHz (filled circles) and 25 MHz (filled diamonds). The curves are from an eyeball fit to the solid phase T_1 data.

Figure 4. Fluid phase fraction, f_L, of ^3He in 2-year-old $PdT_{0.6}$ as a function of temperature.

Figure 5. The dashed curve shows the density distribution for ^3He in 2-year-old PdT_x derived from the fit to the data shown in Fig. 4, using the bulk helium EOS. The solid curve shows the density distribution obtained for ^3He in 8-year-old PdT_x [18].

Figure 6. Age dependence of ^3He fluid phase fraction in palladium tritide; diamonds, 0.55-year-old; triangles, 2-year-old; squares, 4-year-old; circles, 8-year-old. The solid curves are linear fits to the corresponding data.

Figure 7. Excess absorbed tritium (see text for definition) as a function of ^3He concentration. The curve is from a least-squares fit, assuming a 2/3-power law relationship.

Figure 8. ^3He lineshape at 300 K (a) and spin-lattice relaxation time (b) before and after replacement of ^3H by ^2H in $PdT_{0.07}{}^3He_{0.3}$.

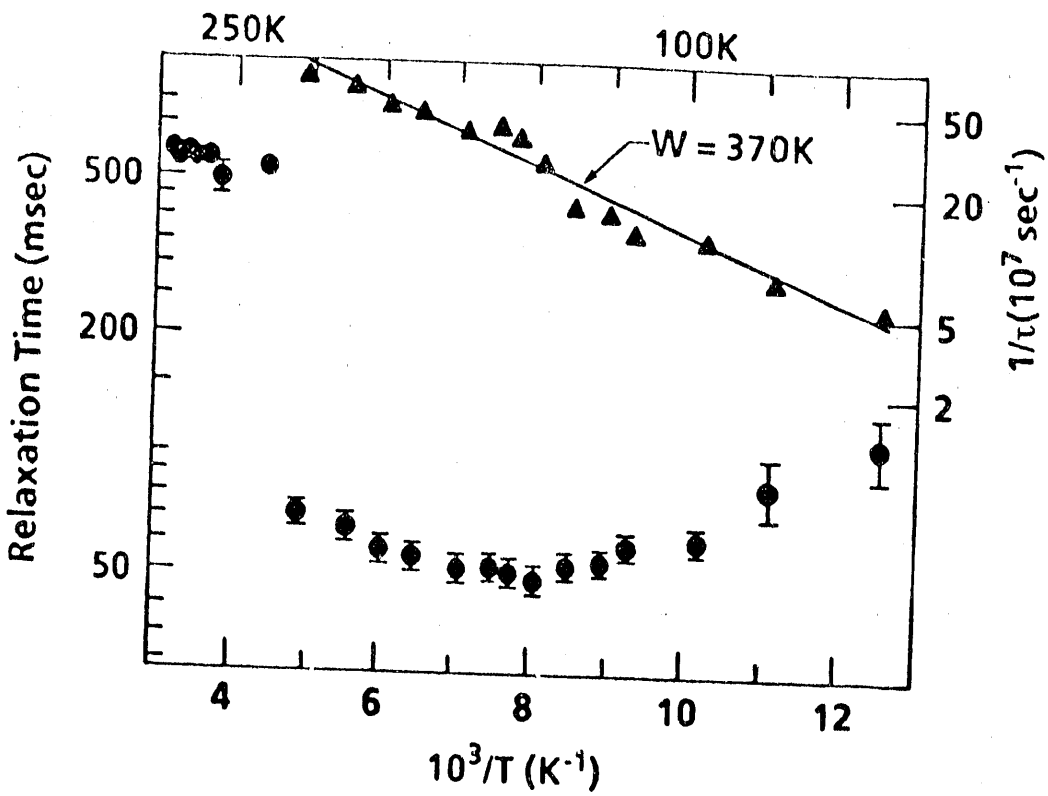

Figure 1. Temperature dependence in 1-year-old $PdT_{0.6}$ of ^3He T_1 relaxation time (filled circles, left-hand scale) at 25 MHz; and of ^3He jump frequency τ^{-1} (filled triangles, right-hand scale) obtained from the T_1 data via eqn. (12).

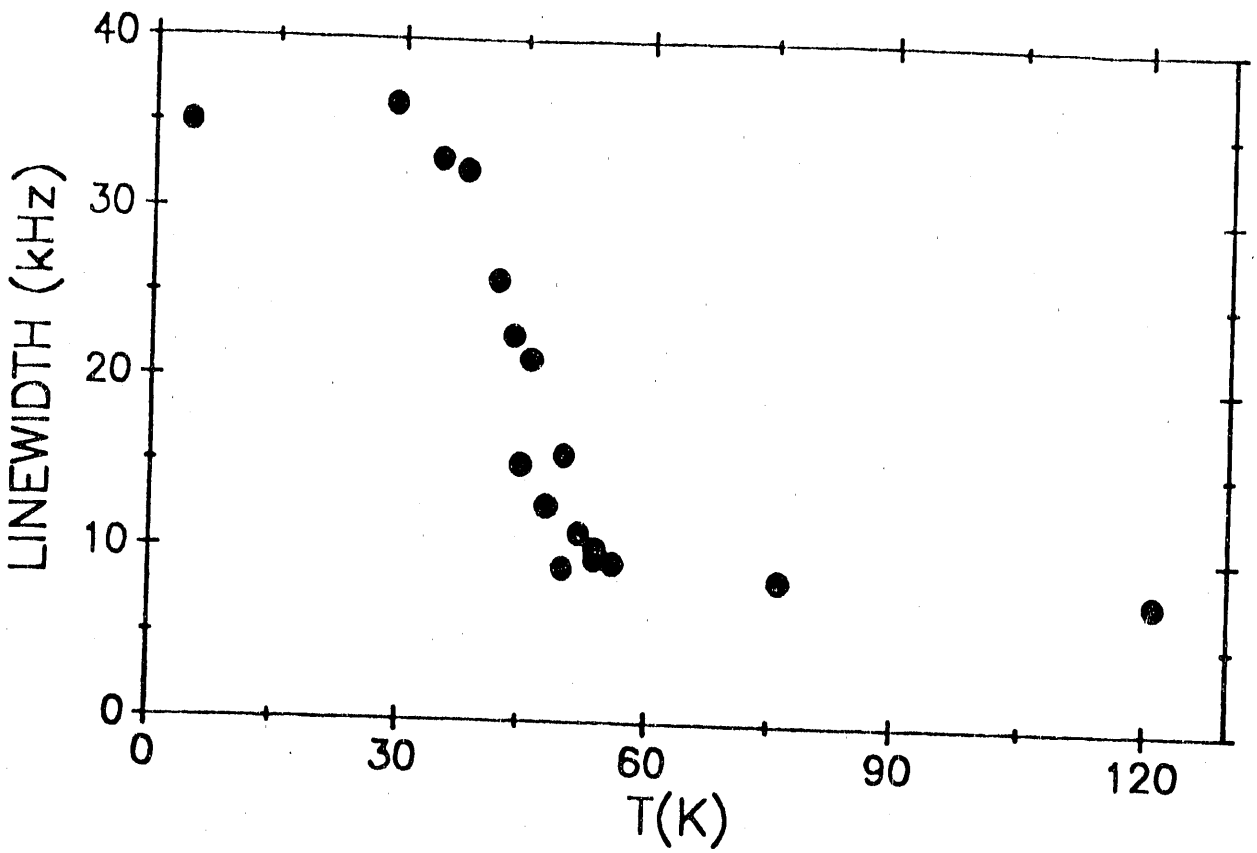

Figure 2. Spectral linewidth of ^{3}He in 8-yr-old PdT_x as a function of temperature ($\omega_0/2\pi$ = 142.8MHz).

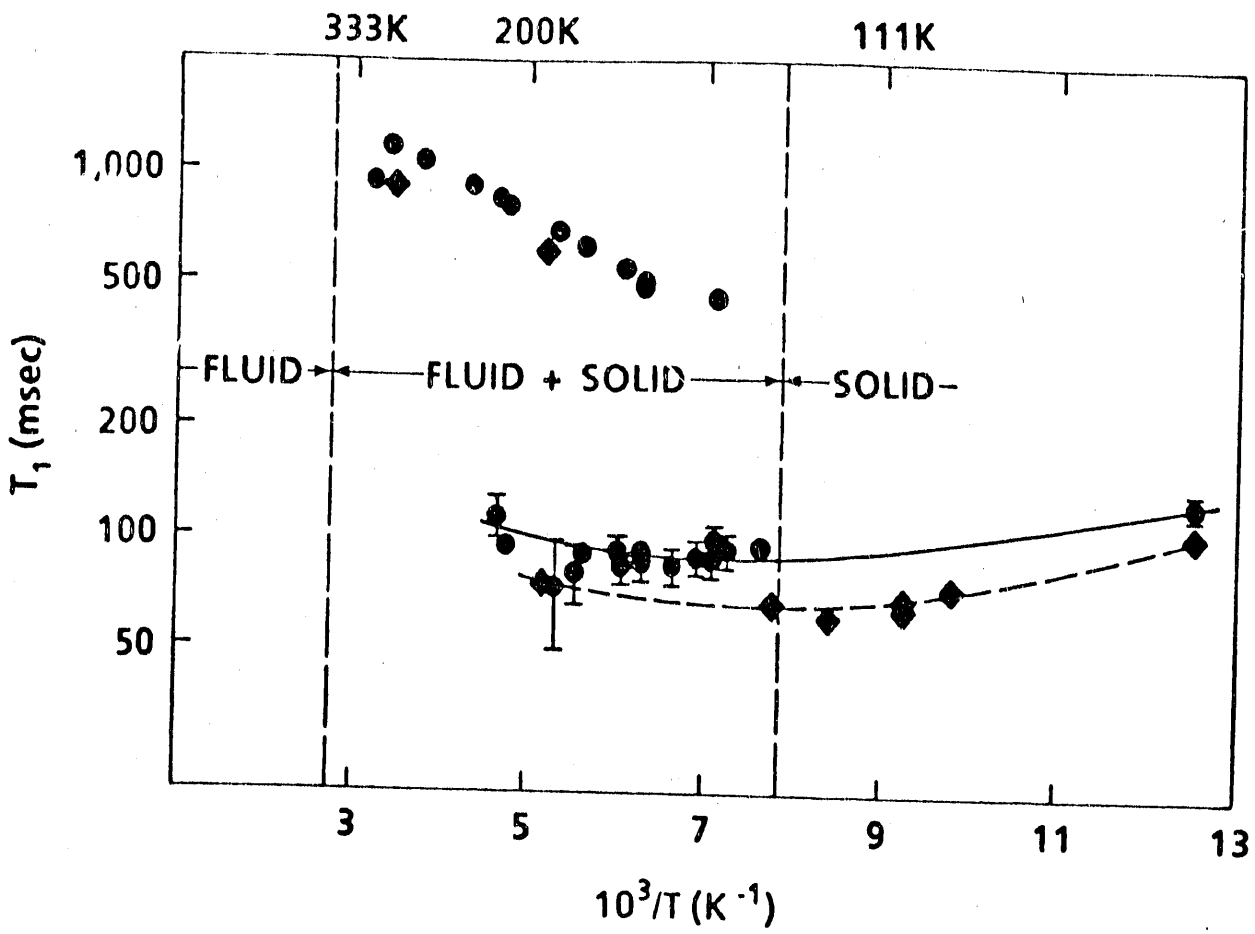

Figure 3. Temperature dependence of ^3He T_1 in 2-year-old $PdT_{0.6}$ at 45.7 MHz (filled circles) and 25 MHz (filled diamonds). The curves are from an eyeball fit to the solid phase T_1 data.

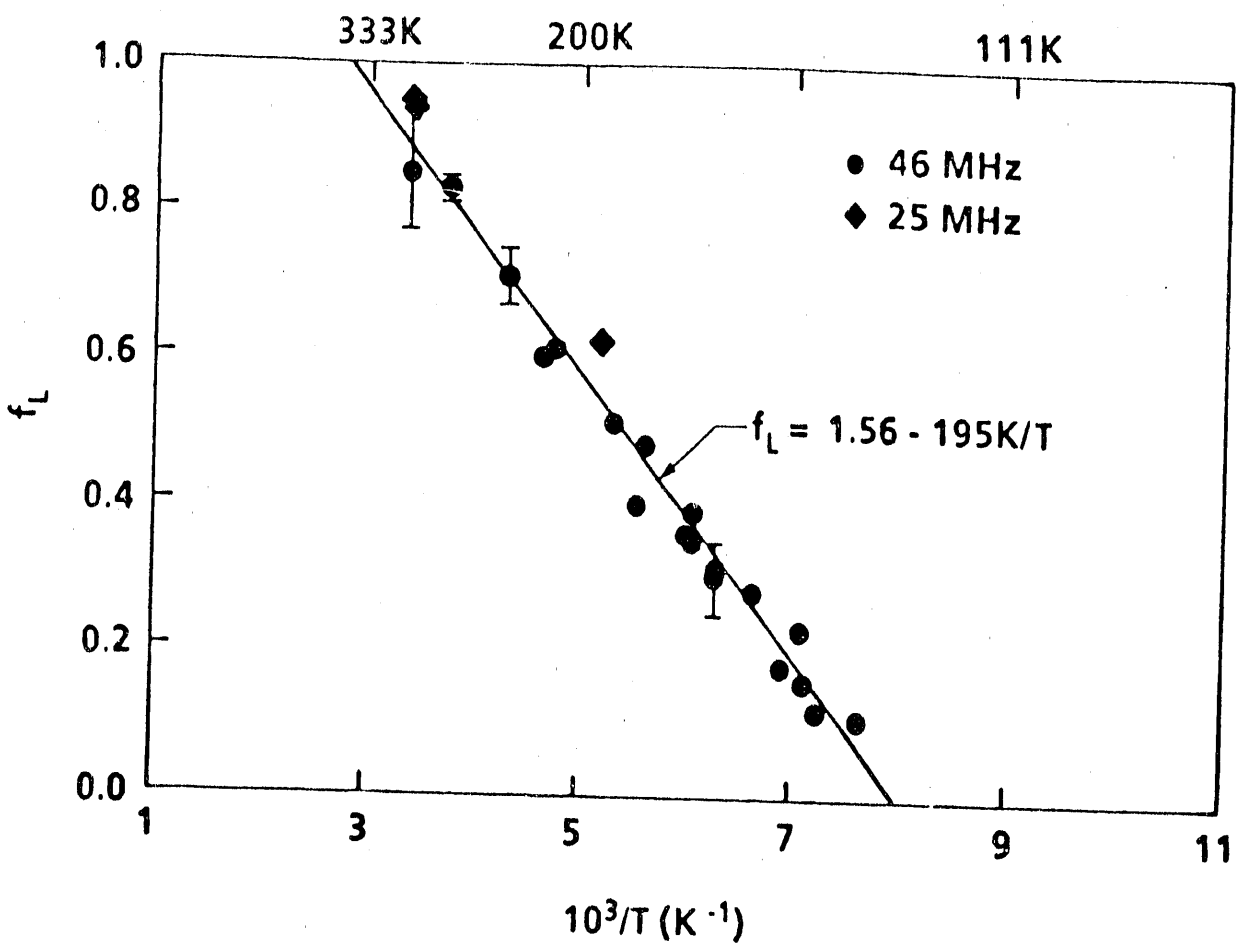

Figure 4. Fluid phase fraction, f_L, of ^3He in 2-year-old $PdT_{0.6}$ as a function of temperature.

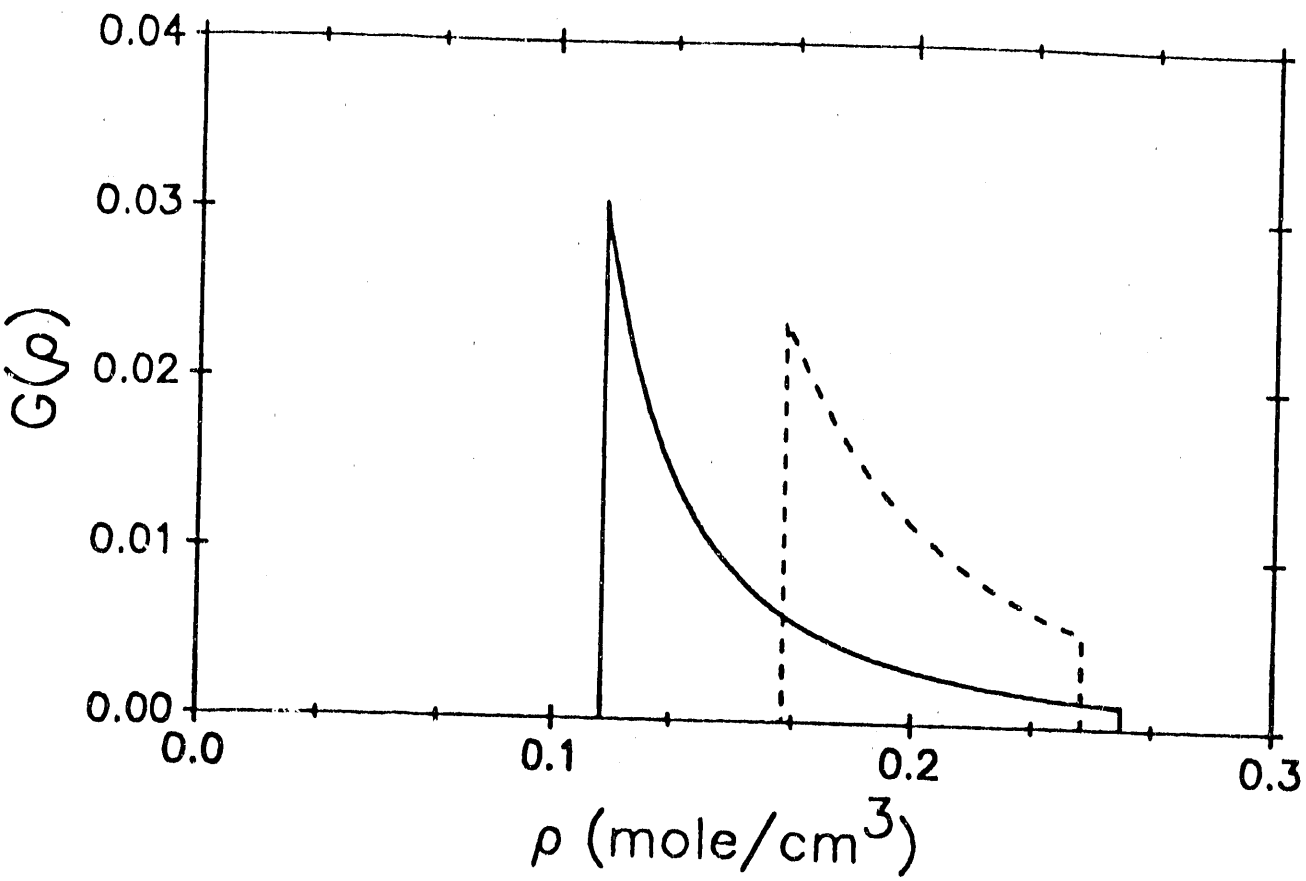

Figure 5. The dashed curve shows the density distribution for ^{3}He in 2-year-old PdT_x derived from the fit to the data shown in Fig. 4, using the bulk helium EOS. The solid curve shows the density distribution obtained for ^{3}He in 8-year-old PdT_x [18].

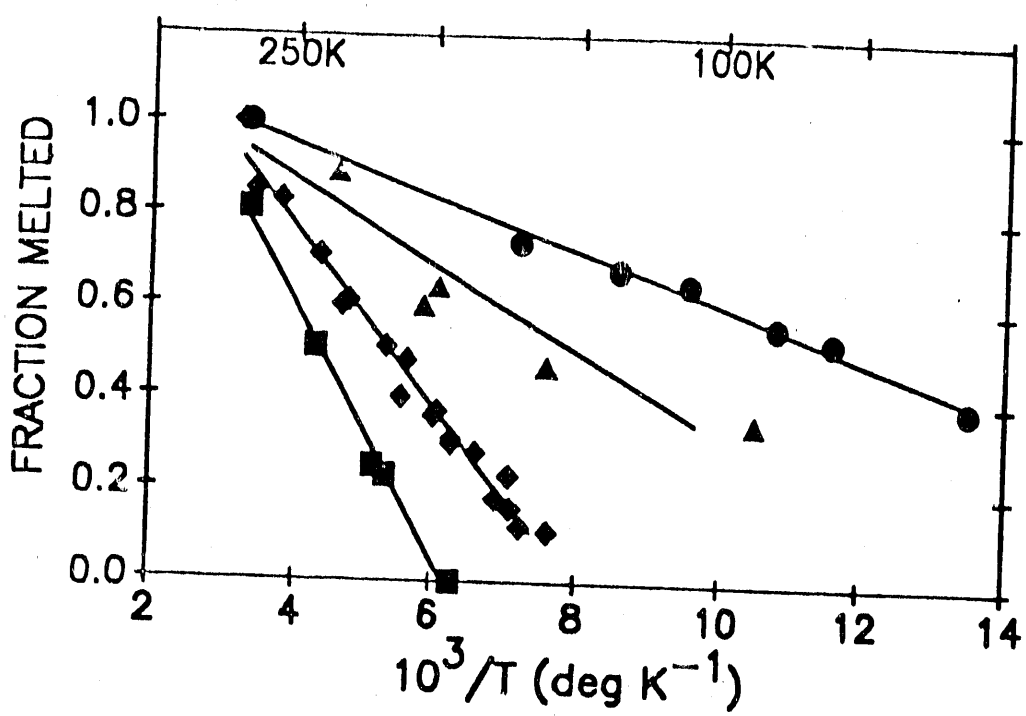

Figure 6. Age dependence of ^3He fluid phase fraction in palladium tritide; diamonds, 0.55-year-old; triangles, 2-year-old; squares, 4-year-old; circles, 8-year-old. The solid curves are linear fits to the corresponding data.

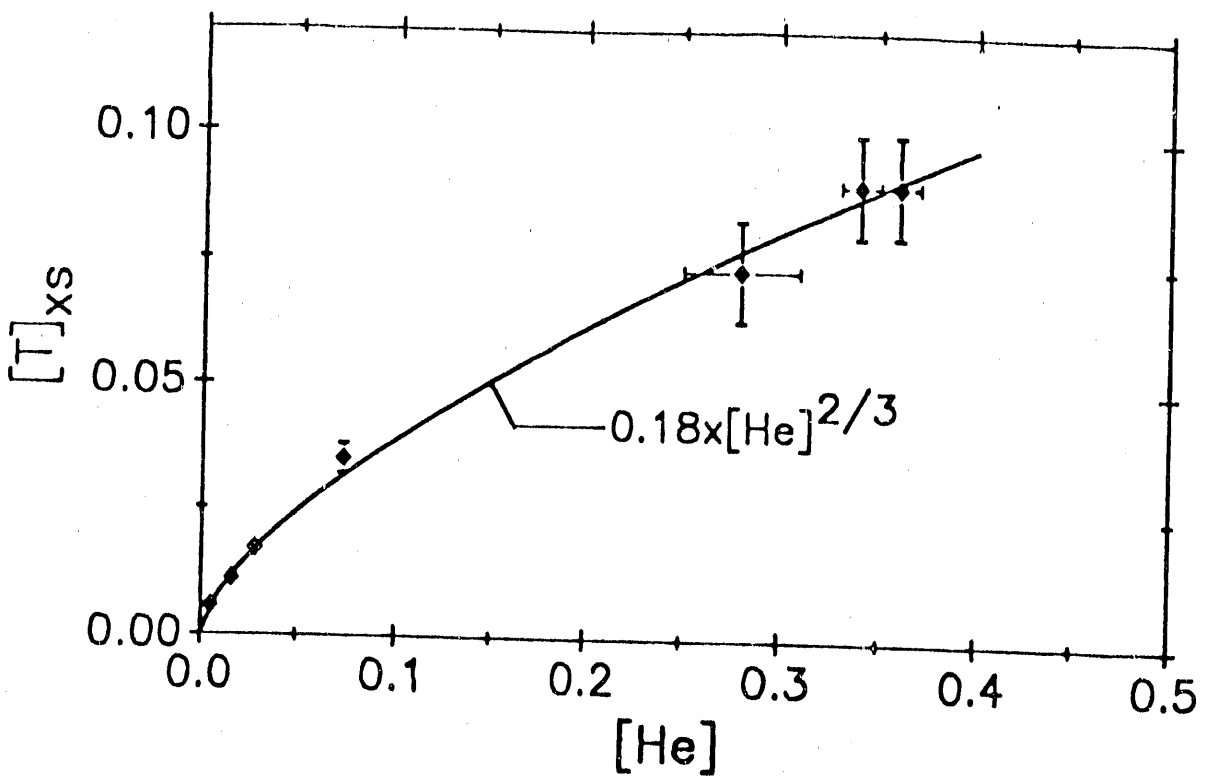

Figure 7. Excess absorbed tritium (see text for definition) as a function of ^{3}He concentration. The curve is from a least-squares fit, assuming a 2/3-power law relationship.

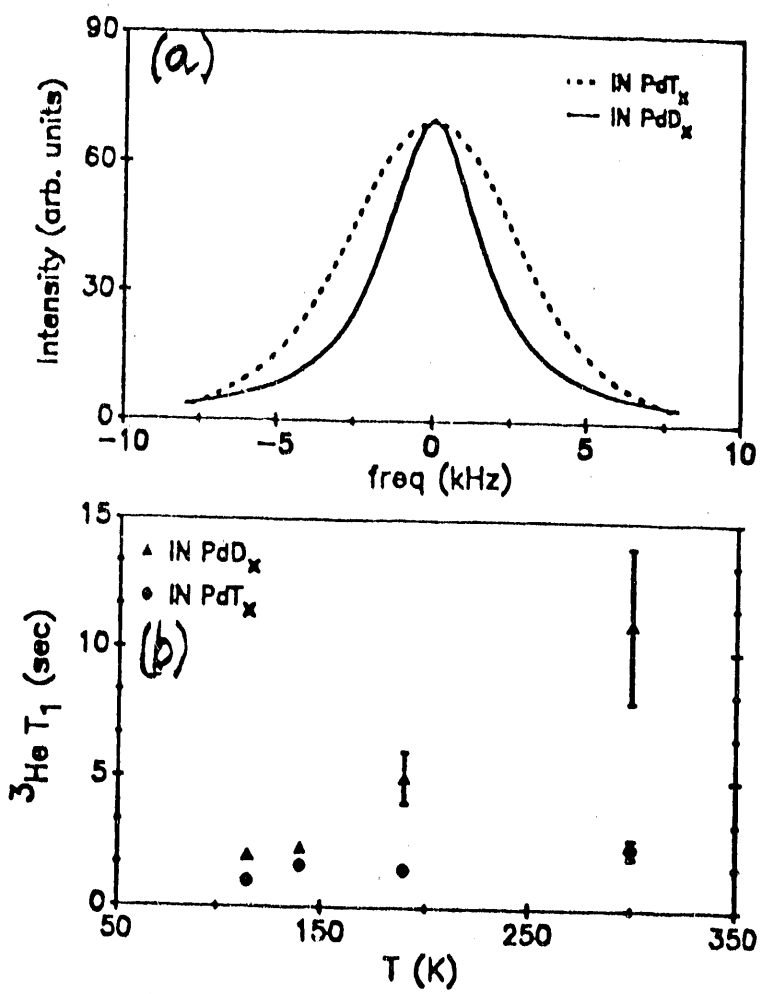

Figure 8. ^{3}He lineshape at 300 K (a) and spin-lattice relaxation time (b) before and after replacement of ^{3}H by ^{2}H in $PdT_{0.07}{}^3He_{0.3}$.

END

DATE FILMED

12/11/90